Selection of CMIP5 general circulation model outputs of precipitation for peninsular Malaysia

Saleem A. Salman, Mohamed Salem Nashwan, Tarmizi Ismail and Shamsuddin Shahid

ABSTRACT

Reduction of uncertainty in climate change projections is a major challenge in impact assessment and adaptation planning. General circulation models (GCMs) along with projection scenarios are the major sources of uncertainty in climate change projections. Therefore, the selection of appropriate GCMs for a region can significantly reduce uncertainty in climate projections. In this study, 20 GCMs were statistically evaluated in replicating the spatial pattern of monsoon propagation towards Peninsular Malaysia at annual and seasonal time frames against the 20th Century Reanalysis dataset. The performance evaluation metrics of the GCMs for different time frames were compromised using a state-of-art multi-criteria decision-making approach, compromise programming, for the selection of GCMs. Finally, the selected GCMs were interpolated to $0.25^\circ \times 0.25^\circ$ spatial resolution and bias-corrected using the Asian Precipitation – Highly-Resolved Observational Integration Towards Evaluation (APHRODITE) rainfall as reference data. The results revealed the better performance of BCC-CSM1-1 and HadGEM2-ES in replicating the historical rainfall in Peninsular Malaysia. The bias-corrected projections of selected GCMs revealed a large variation of the mean, standard deviation and 95% percentile of daily rainfall in the study area for two futures, 2020–2059 and 2060–2099 compared to base climate.

Key words | climate change, compromise programming, general circulation model, model selection

Saleem A. Salman
Mohamed Salem Nashwan
Tarmizi Ismail (corresponding author)
Shamsuddin Shahid
School of Civil Engineering, Faculty of Engineering,
Universiti Teknologi Malaysia,
81310 Johor Bahru,
Malaysia
E-mail: *tarmiziismail@utm.my*

Mohamed Salem Nashwan
Department of Construction and Building Engineering, College of Engineering and Technology,
Arab Academy for Science,
Technology and Maritime Transport (AASTMT),
2033 Elhorria, Heliopolis, Cairo,
Egypt

INTRODUCTION

The uncertainties in climate projections heavily influence the quantification of impacts (Deser *et al.* 2012). A slight variation in the changes in climate projection can significantly change the return period of hydrological disasters such as flood, droughts, etc. (Camici *et al.* 2014; Qin & Lu 2014; Nashwan *et al.* 2019b). The reduction of uncertainty in climate change projection is considered as the major challenge in climate change studies (Shiogama *et al.* 2016; Lehner *et al.* 2019). A number of approaches have been proposed in the literature for quantification and reduction of uncertainty arising from general circulation models (GCMs) and emission scenarios (Shiogama *et al.* 2016; Hosseinzadehtalaei *et al.* 2017; Mateus & Tullos 2017; Kaczmarska *et al.* 2018; Satoh *et al.* 2018; Lehner *et al.* 2019). Most of the methods are based on the departure of the GCMs from their ensemble mean. The major disadvantage of existing approaches is that they under- or over-estimate the uncertainty in projection, particularly uncertainty in extreme weather events. The return period of extreme events heavily depends on climate variability rather than climatic mean and therefore, uncertainty in climate projections heavily under- or overestimate the return periods of extremes (Harris *et al.* 2013; Hewitt *et al.* 2016). Consequently, development and planning activities based on projected climate suffers from a high risk of failure. This emphasizes the

doi: 10.2166/nh.2020.154

need for more study on the reduction of uncertainty in climate projections. A number of studies have been conducted for the reduction of uncertainty in climate projections in different climatic and geographical regions (Mateus & Tullos 2017; Kaczmarska *et al.* 2018).

Uncertainty in climate change projections arises from different sources including GCMs, climate change scenarios, and downscaling techniques (Ahmed *et al.* 2019; Sachindra *et al.* 2019). However, errors in the model structure, adopted initial conditions, calibration procedure, calibration data and representation of the atmospheric and other processes in GCM development are the main sources of uncertainties (Pour *et al.* 2018; Sachindra *et al.* 2018; Ahmed *et al.* 2019). Therefore, selection of credible GCMs is considered as one of the effective ways in reducing the uncertainty in climate change projections (Salman *et al.* 2018; Sa'adi *et al.* 2019; Shiru *et al.* 2019).

GCMs are generally selected according to their ability to simulate historical climate (Lutz *et al.* 2016). Mostly, time series of monthly or annual observed and GCM simulated climate are compared to assess the performance of GCMs. Selection of GCMs by conventional approach provides emphasis on their ability to simulate temporal variability in rainfall (Ahmed *et al.* 2019; Noor *et al.* 2019b). The ability of GCMs in simulating spatial variability in climate is often ignored although it has similar importance. Besides, GCMs are also selected based on their capability to simulate large-scale ocean-atmospheric phenomena responsible for climate variation of a region. For example, the ability of GCMs to simulate monsoon is very important to show its capability to project rainfall in a monsoon-dominated rainfall region. This emphasizes the need for selection of GCMs for a region according to their ability to simulate the propagation of large-scale ocean-atmospheric phenomena that determine the climate of the region.

Various statistics have been used in previous studies for the evaluation of the performance of GCMs such as correlation, root mean square error (RMSE), mean absolute error (MAE), standard deviation ratio, etc. (Lutz *et al.* 2016; Nashwan & Shahid 2019; Noor *et al.* 2019a). Evaluation and selection of credible GCMs based on single statistical metrics are questionable and not common (Raju *et al.* 2017). This is because each metric measures only a certain characteristic of the GCMs time series compared to the reference time series (Weigel *et al.* 2010; McSweeney *et al.* 2015). Thus, a bundle of statistics is commonly used to evaluate the performance of GCMs in a region (Johnson & Sharma 2009). Nevertheless, the problem of contradictory results often arises when different metrics are used (Raju *et al.* 2017; Nashwan *et al.* 2018b). For example, two pairs of time series can have high R^2 indicating high correlation even if the error between them is high. Furthermore, the RMSE can have a near-optimal value even if a pair of time series does not follow the same variability. In such a case, the compromise programming (CP), developed by Zeleny (1973), can be helpful in determining the most credible subset of GCMs by judicious compromising different objectives of which some may be contradicting or conflicting (Rezaei *et al.* 2017; Salman *et al.* 2019). CP is a technique for estimating the minimum distance between the efficient frontier and the ideal point based on the level of importance assigned to each criterion (Muhammad *et al.* 2019). By applying CP, a subset of GCMs can be identified which can achieve the considered objectives in a compromised manner. CP has been used previously for the selection of GCMs (Raju *et al.* 2017; Salman *et al.* 2019) and was found efficient compared to the conventional multi-criteria decision-making methods in other fields of study (Chen *et al.* 1999; Gorantiwar & Smout 2010).

Although a large number of studies have been conducted for selection of GCMs in different parts of the world using different approaches for reliable projections of climate, there is almost no study in Peninsular Malaysia. The only attempt taken for selection of GCMs in Peninsular Malaysia was by Noor *et al.* (2019b). They compared the GCM historical simulated rainfall with the Asian Precipitation – Highly-Resolved Observational Integration Towards Evaluation (APHRODITE) rainfall for the period 1961–2005 using five statistical metrics for the ranking of GCMs according to their ability to simulate the APHRODITE rainfall. They selected four GCMs, BCC-CSM1.1(M), CCSM4, CSIRO-Mk3.6.0, and HadGEM2-ES as the most suitable GCMs for the projection of daily rainfall of Peninsular Malaysia. However, the ability of GCMs not only depends on their ability to simulate the temporal variability of rainfall, but mainly according to their ability to simulate large-scale phenomena like the propagation of monsoons, which was ignored in the study of Noor *et al.* (2019b).

The objective of the present study is to select the most credible set of GCMs based on their ability in the simulation of monsoon in the region for the projection of rainfall in Peninsular Malaysia. Six statistical metrics were used in CP for the selection of GCMs based on their ability to replicate the spatial variability of monsoon rainfall pattern in the region. The daily rainfall projections of the selected GCMs for different radiative concentration pathway (RCP) scenarios were downscaled and compared to base period rainfall (1971–2000) to show the possible future changes in two futures, 2020–2059 and 2060–2099.

STUDY AREA AND DATA

Study area

Peninsular Malaysia (latitude 1°15′–6°45′N and longitude 100°–104°30′E) (Figure 1) has an equatorial climate characterized by uniform temperature, high humidity, and copious rainfall (Sa'adi *et al.* 2017; Nashwan *et al.* 2019a). Daily temperature ranges from 23 °C in the early morning to 32 °C at noon. Humidity is constantly high and usually exceeds 68% throughout the year (Muhammad *et al.* 2019). The peninsula experiences two monsoons which are influenced by seasonal wind flow, namely, northeast (NEM) and southwest (SWM) and two short inter-monsoon seasons in April and October (Noor *et al.* 2018). The NEM is more prominent because of the sudden surge in the rainfall amounts while the SWM is associated with a relatively dry period during the active monsoon months May to August (Pour *et al.* 2014; Mayowa *et al.* 2015; Shahid *et al.* 2017; Nashwan *et al.* 2018a).

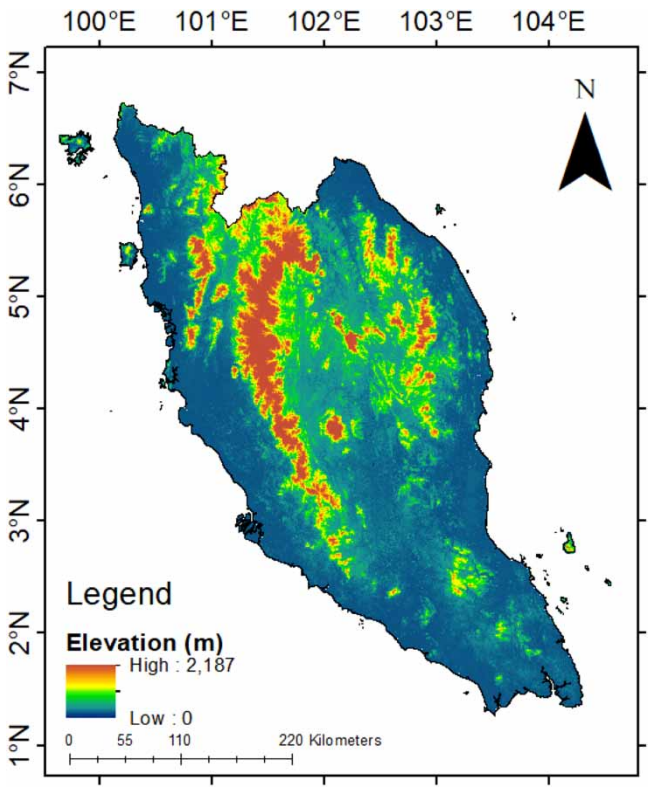

Figure 1 | Peninsula Malaysia location and topography.

Data used

Two groups of datasets were used in this study. The first group includes the 20th Century Reanalysis (20CR) version 2 and the Asian Precipitation – Highly-Resolved Observational Data Integration Towards Evaluation (APHRODITE), and the second includes 20 CMIP5 GCMs. The 20CR dataset provides monthly average estimations of rainfall in spatial coverage of $2^\circ \times 2^\circ$ over both land and ocean, thus it can represent large-scale monsoon propagation towards the study area. Therefore, 20CR was used as a reference dataset to assess the capabilities of different GCMs in simulating rainfall in three time frames, annual, NEM and SWM. The 20CR data were extracted for a study domain (latitude: −12.5 to −21.0° and longitude: 80.0–121.5°) centred on the Malaysian Peninsula. This study domain was selected to reflect the propagation of both NEM and SWM in the study area. Figure 2 presents the spatial distribution of monsoon rainfall estimated by 20CR data during 1961–2005 over the study domain. The NEM rainfall in the Southeast Asia region varies between 0 mm in the east and north and 350 mm in Borneo and some parts of the China Sea. The SWM varies between the maximum rainfall of 400 mm in the north of the region and 0 mm in the south. A distinct pattern in the propagation of NEM and SWM can be found in Peninsular Malaysia.

On the other hand, APHRODITE provides daily estimates of rainfall on a $0.25^\circ \times 0.25^\circ$ spatial grid over land

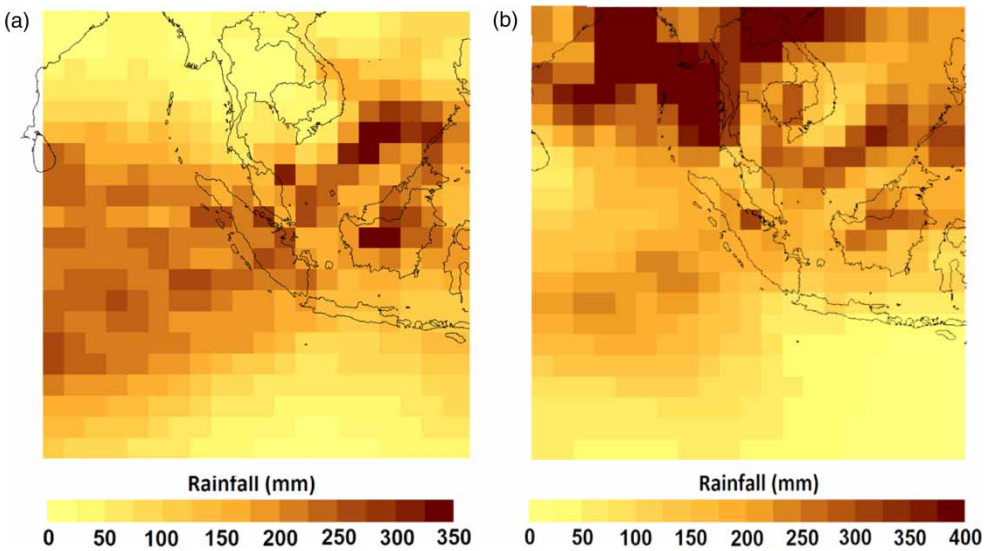

Figure 2 | The (a) NEM and (b) SWM rainfall variation estimated by the 20CR precipitation dataset for the period 1961–2005.

only. It has been developed using nearly 12,000 gauges covering Asia (Yatagai *et al.* 2012). Owing to its fine spatial and temporal resolution, APHRODITE was used as a reference dataset to statistically downscale the selected subset of GCMs at fine resolution. APHRODITE has been widely used to represent rainfall in Malaysia and nearby countries (Yen *et al.* 2011; Chen *et al.* 2013; Le Loh *et al.* 2016). Studies have also reported good performance of APHRODITE in estimating the spatial and the temporal variability of rainfall in the study area (Noor *et al.* 2019b; Pour *et al.* 2020). Tan *et al.* (2015) evaluated the performance of APHRODITE against numerous gauge data and found that it can estimate NEM and SWM rainfall amount more accurately than five other satellite precipitation products. Furthermore, Tan *et al.* (2017) found that APHRODITE rainfall estimates can accurately generate streamflow simulations in Malaysia. Noor *et al.* (2019b) used APHRODITE as a reference dataset to select a multi-model ensemble for the projection of rainfall in Peninsular Malaysia.

Out of more than 45 GCMs available in CMIP5, 20 GCMs were initially selected in this study as they have daily historical data (1961–2005) and future projections (2020–2099) for the four RCPs (i.e., 2.6, 4.5, 6.0 and 8.5) to cover a wide range of possible future changes. The GCM name, modelling centre and spatial resolution are provided in Table 1.

METHODOLOGY

Procedure

The procedure of selecting and bias-correcting a subset of GCMs for reduction of uncertainty in rainfall projection for Peninsular Malaysia is outlined below:

1. The CMIP5 GCMs' rainfall simulations were interpolated onto a common resolution of $2.00^\circ \times 2.00^\circ$ using bilinear interpolation.
2. The performances of GCMs in simulating the spatial variability of rainfall at the annual, NEM and SWM time frames over the study domain were assessed using statistical metrics against 20CR estimates as reference dataset during 1961–2005.
3. The CP was used to rank the GCMs based on the statistical metrics results of different GCMs for each time frame separately.
4. The GCMs ranked above 50th percentile (i.e., ranks 1–10) for each time frame were selected considering that they are capable to simulate the spatial variability of each time frame rainfall over the study domain.
5. The selected GCMs' simulations of rainfall were interpolated to $0.25^\circ \times 0.25^\circ$, the same as the resolution of APHRODITE, using bilinear interpolation over Peninsular Malaysia.

Table 1 | List of CMIP5 GCMs used in the study

Model	Modelling centre	Resolution (Long. × Lat.)
BCC-CSM1.1(m)	Beijing Climate Center, China	2.80° × 2.80°
BCC-CSM1 – 1		2.80° × 2.80°
CanESM2	Canadian Centre for Climate Modelling and Analysis, Canada	2.80° × 2.80°
CCSM4	National Center for Atmospheric Research, USA	1.25° × 0.94°
CMCC-CM	Centro Euro-Mediterraneo sui Cambiamenti Climatici, Italy	0.75° × 0.75°
CMCC-CMS		3.75° × 3.71°
CNRM-CM5	Centre National de Recherches Météorologiques, Centre Européen de Recherche et de Formation Avancée en Calcul Scientifique, France	1.40° × 1.40°
CSIRO-Mk3.6.0	Commonwealth Scientific and Industrial Research Organization/Queensland Climate Change Centre of Excellence, Australia	1.86° × 1.87°
GFDL-CM3	Geophysical Fluid Dynamics Laboratory, USA	2.50° × 2.01°
GISS-E2-H	NASA/GISS (Goddard Institute for Space Studies), USA	2.50° × 2.50°
HadGEM2-AO	Met Office Hadley Centre, UK	1.25° × 1.87°
HadGEM2-ES		1.87° × 1.25°
INMCM4.0	Russian Academy of Sciences, Institute of Numerical Mathematics, Russia	2.00° × 1.50°
MIROC5	Atmosphere and Ocean Research Institute, The University of Tokyo, Japan	1.40° × 1.40°
MIROC-ESM		2.80° × 2.80°
MIROC-ESM-CHEM		2.80° × 2.80°
MPI-ESM-LR	Max Planck Institute for Meteorology, Germany	1.87° × 1.86°
MPI-ESM-MR		1.87° × 1.86°
NorESM1-M	Bjerknes Centre for Climate Research, Norwegian Meteorological Institute, Norway	2.50° × 1.90°
NorESM1-M		2.50° × 1.90°

6. The biases in the selected GCMs' simulations were corrected using linear scaling method by using APHRODITE as a reference dataset for the historical period.
7. The bias-correction factors were then applied to correct the bias in the projected estimates of the selected GCMs for the four RCPs.

The bias-corrected rainfall estimated by the selected GCMs were used to show the spatial and temporal changes in the mean, standard deviation and 95th percentile of the daily rainfall during the near and far futures (2020–2059 and 2060–2099, respectively) compared to a base period (1971–2000). Details of the methods are discussed below.

Statistical evaluation of GCM outputs

Six statistical metrics were used to evaluate the performance of the GCMs in simulating spatial variability of rainfall at three time frames (i.e., annual, NEM and SEM), separately, against the 20CR rainfall for the historical period 1961–2005. First, GCM data were interpolated to 20CR spatial resolution using the bilinear interpolation method. The bilinear interpolation method was used as it can smoothly interpolate GCMs without changing the climate signal. The interpolated GCM and 20CR rainfall data for the period 1961–2005 at each grid point were then averaged to show the spatial variability of GCM and 20CR rainfall. The average values of GCM and 20CR rainfall at different grid points were compared using six statistical metrics, percentage of bias (Pbias), normalized root mean square error (NRMSE), Nash–Sutcliffe efficiency (NSE), modified index of agreement (md), the coefficient of determination (R^2) and the ratio of standard deviation (rSD). The Pbias measures the tendency of model data to over- or under-estimate the observed data. The NRMSE summarizes the magnitudes of the errors in

predictions for various times and is, therefore, considered a good measure of accuracy (Willmott 2013). The NSE is a normalized statistic that determines the relative magnitude of the residual variance compared to the reference data variance (Nash & Sutcliffe 1970). The md can detect additive and proportional differences in the reference and estimated means and variances. The R^2 measures the correlation and rSD measure the ratio of standard deviations between the simulated and reference time series. Table 2 presents each metric equation and its optimal value. Here, the GCMs and 20CR estimation is indicated by $x_{sim,i}$ and $x_{obs,i}$, respectively, of data pair i and n is the total number of data pairs.

Compromise programming for ranking the GCMs

Ranking the GCMs of different statistical evaluation results for different time frames is a challenging task due to the fact that a GCM may show various degrees of under/overestimations of a climatic variable for different time frames (Nashwan & Shahid 2020). Thus, CP was used to integrate the historical evaluation results of GCMs to enable their ranking for each time frame. The CP measures the distance (Lcp) of each GCM from an ideal value or frontier (Zeleny 1973; Gorantiwar & Smout 2010) and uses this distance to rank the GCMs. The Lcp is estimated as follows:

$$\mathrm{Lcp} = \left[\sum_{j=1}^{z} |x_j - x_j*|^p\right]^{1/p} \quad (7)$$

where z is the number of evaluation metrics used, x_j is the normalized value of metric j obtained for a certain GCM, x_j^* is the normalized ideal value of the metric j, and p is the parameter (1 for linear, and 2 for squared Euclidean distance measure). In the present study, the linear measure was used and, therefore, the value of p was considered equal to 1. The Lcp can have any positive value whereas the low Lcp as zero indicates the closeness of a GCM simulation of rainfall to the 20CR simulation. This study gave equal importance to all GCMs and metrics, therefore no weight was given as proposed by Zeleny (1973). The Lcp results were used to rank the GCMs in estimating the seasonal and annual rainfall where the GCMs which scored the lowest Lp were given the first rank and vice versa.

Table 2 | Statistical metrics used for evaluation of GCMs

Equation		Optimal value
$Pbias = 100 \times \left[\frac{\sum_{i=1}^{n}(x_{sim,i} - x_{obs,i})}{\sum_{i=1}^{n} x_{sim,i}}\right]$	(1)	0
$NRMSE = \frac{\left[\frac{1}{n}\sum_{i=1}^{n}(x_{sim,i} - x_{obs,i})^2\right]^{\frac{1}{2}}}{\frac{1}{n}\sum_{i=1}^{n}(x_{sim,i})}$	(2)	0
$NSE = 1 - \frac{\sum_{i=1}^{n}(x_{sim,i} - x_{obs,i})^2}{\sum_{i=1}^{n}(x_{obs,i} - \overline{x_{obs}})^2}$	(3)	1
$md = 1 - \frac{\sum_{i=1}^{n}(x_{obs,i} - x_{sim,i})^j}{\sum_{i=1}^{n}(\lvert x_{sim,i} - \overline{x_{obs}}\rvert + \lvert x_{obs,i} - \overline{x_{0bs}}\rvert)^j}$	(4)	1
$R^2 = \frac{\sum_{i=1}^{n}(x_{obs,i} - \overline{x_{obs}})(x_{sim,i} - \overline{x_{sim}})}{\sqrt{\sum_{i=1}^{n}(x_{sim,i} - \overline{x_{sim}})^2}(x_{obs,i} - \overline{x_{obs}})^2}$	(5)	1
$rSD = \frac{SD\,(x_{sim})}{SD\,(x_{obs})}$	(6)	1

Selection of GCMs

Ahmed *et al.* (2020) evaluated the performance of multi-model ensemble (MME) developed with different combinations of GCMs ranked based on their performance and the determination of the optimum number of GCMs to be included in an MME. They introduced as a rule of thumb that the optimum performance of MMEs can be achieved when about 50% of the top-ranked GCMs are used in the MME as its performance did not achieve significant improvements with the addition of more GCMs. Nashwan & Shahid (2020) used this rule of thumb for the selection of GCMs in estimating three climate variables for Egypt. In this study, the same rule of thumb was adopted.

As both rainfall seasons are equally important for Peninsular Malaysia, the GCMs which are capable of accurately simulating both seasons as well as annual are favourable. The final selection of GCMs is expected to perform well in reproducing the rainfall time series for the three time frames. Therefore, following Khan *et al.* (2018), Ahmed *et al.* (2020) and Nashwan & Shahid (2020), the rule of thumb 'a GCM

having a rank lower than the 50th percentile (i.e., rank ≥ 10) in simulating either annual and seasonal rainfall is not suitable for rainfall projections of Peninsular Malaysian' was applied.

Bias correction of GCMs and future projection of daily rainfall

Selected GCMs were re-gridded to a resolution of 0.25° × 0.25° which complies with the resolution of APHRODITE. The linear scaling method was used to correct the bias in GCM simulated daily rainfall based on APHRODITE rainfall for the period 1961–2005 at each grid point. Linear scaling is one of the most widely used methods to correct the bias in GCM outputs because of its simplicity and accuracy (Aqilah Tukimat 2018). It has been found effective compared to many other methods in a number of studies (Noor *et al.* 2019b; Shiru *et al.* 2019). The linear scaling method aims to match the monthly mean of GCM rainfall with the monthly mean of observed rainfall perfectly (Lenderink *et al.* 2007; Fang *et al.* 2015) through the use of the following equation:

$$R_{cor,m,d} = R_{raw,m,d} \times \left[\frac{\mu(R_{obs,m})}{\mu(R_{raw,m})}\right] \quad (8)$$

where $R_{cor,m,d}$ is the corrected rainfall data of the d-th day of the m-th month, is the raw GCM interpolated data for the same day, and $\mu(R_{obs,m})$ and $\mu(R_{raw,m})$ are the monthly mean of observed and raw GCM data of the m-th month, respectively.

Then, the bias correction factors were used to correct the bias of the projected rainfall of the selected GCMs. Afterwards, the bias-corrected future data of the selected GCMs for the four RCPs were compared to the base period (1971–2000) to analyse the change in the mean, standard deviation and 95th percentile of the daily rainfall during two futures (near future: 2020–2059 and far future: 2060–2099). ArcGIS v.10.3 was used to plot the maps of projected changes.

RESULTS AND DISCUSSION

Monsoon simulations by GCMs

Figures 3 and 4 show the spatial pattern of the simulated NEM and SWM mean rainfall, respectively, by 20 GCMs for the historical period 1961–2005 over the study domain. Overall, the GCMs were able to capture the spatial distribution of rainfall during the two main rainy seasons, however, with under- or overestimation compared to the reference 20CR data. The observed NEM mean rainfall pattern, including the elongated rain belt along the Intertropical Convergence Zone near 20°N, the South Pacific Convergence Zone over the western Pacific and the rain associated with the convergence zone over the central and eastern equatorial Indian Ocean were reasonably represented by most GCMs. A common positive rainfall bias over the southwest Indian Ocean was present in most of these GCM simulations.

Statistical evaluation of GCMs' outputs

The statistical evaluation results of the 20 GCMs against the reference data of 20CR for annual, NEM and SWM time frames using the six metrics are presented in Figure 5 as box and whiskers plots. At each time frame, the GCMs showed a distinct performance as evidenced by the median value of the corresponding metric and the spread of the results. Overall, the GCMs' historical estimates of the NEM rainfall were more accurate than SWM and annual rainfall in term of medians of NRMSE%, NSE, md and R^2 (i.e., 75%, 0.45, 0.66 and 0.52, respectively). However, the GCMs underestimated the NEM rainfall by a median of 9.00% bias, as shown in Figure 5(a). The median rSD at the annual time frame was closer to the optimal one than at NEM and SWM.

Compromise programming and models ranking

In order to decide and select the near-optimum GCMs based on the statistical metrics results, CP was used to estimate the distance of each GCM from the ideal point. In this study, the nearest to the optimal value of a statistical matric (i.e., the lowest NRMSE%, the highest NSE, md and R^2, the nearest rSD to 1, and the nearest Pbias to 0) was used as the ideal value of the corresponding metric. Table 3 shows the results of the statistical metrics of each GCM for the NEM evaluation. The bottom row of the table shows the ideal value of each metrics. Following the methodology described earlier, the Lcps were calculated

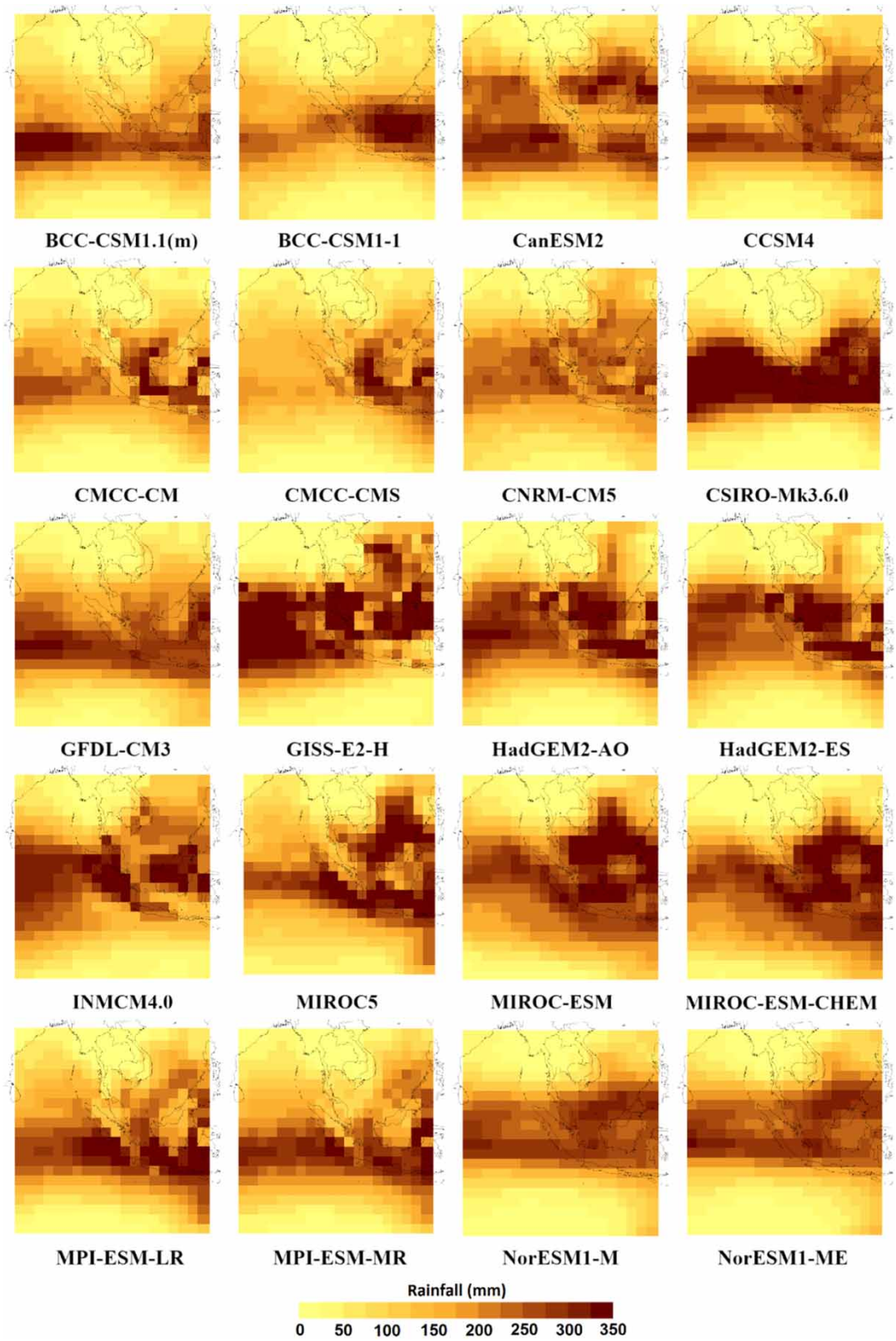

Figure 3 | Mean of daily rainfall of NEM during the historical period of 1961–2005 simulated by different GCMs.

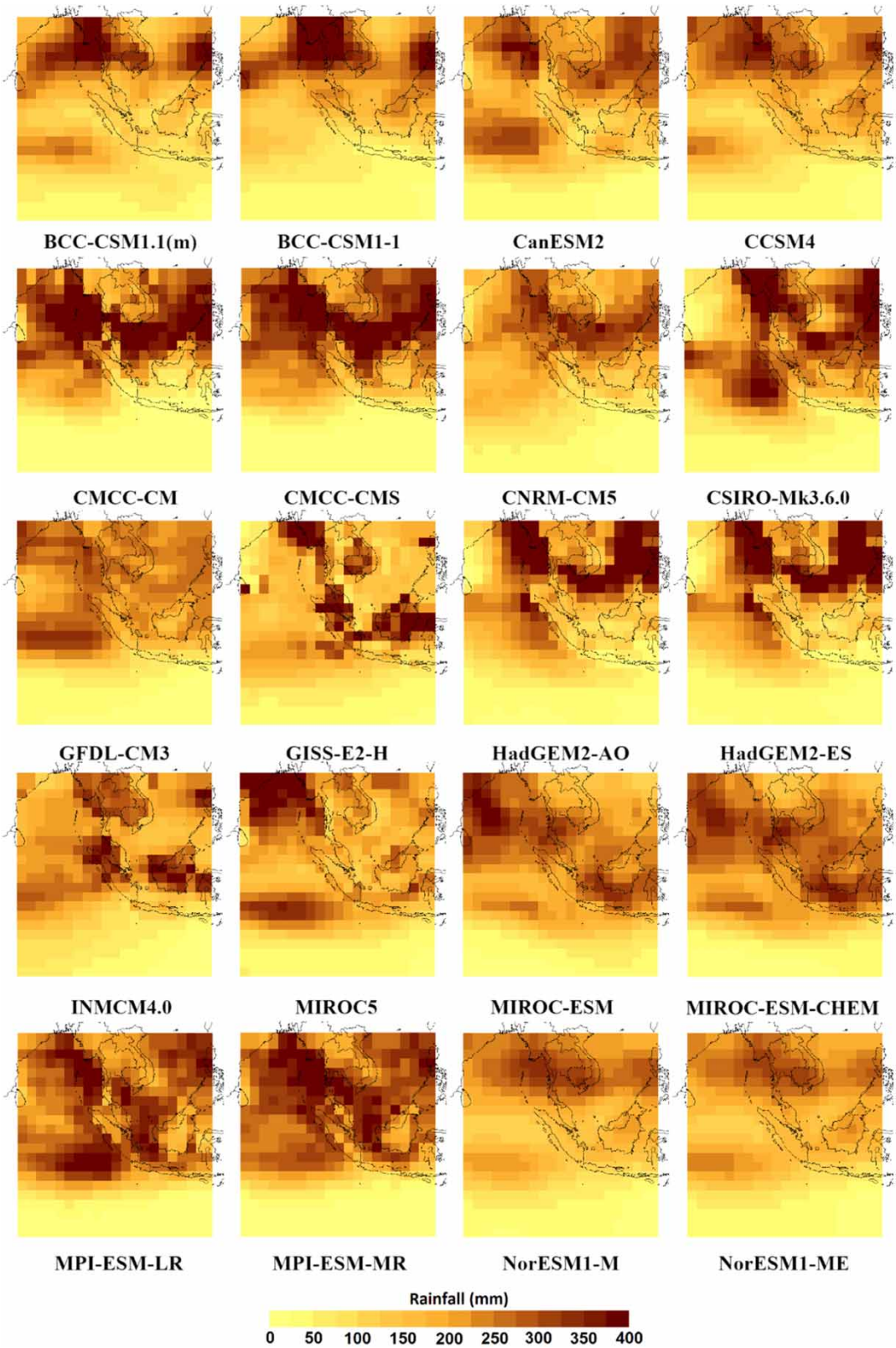

Figure 4 | Mean of daily rainfall of SWM during the historical period of 1961–2005 simulated by different GCMs.

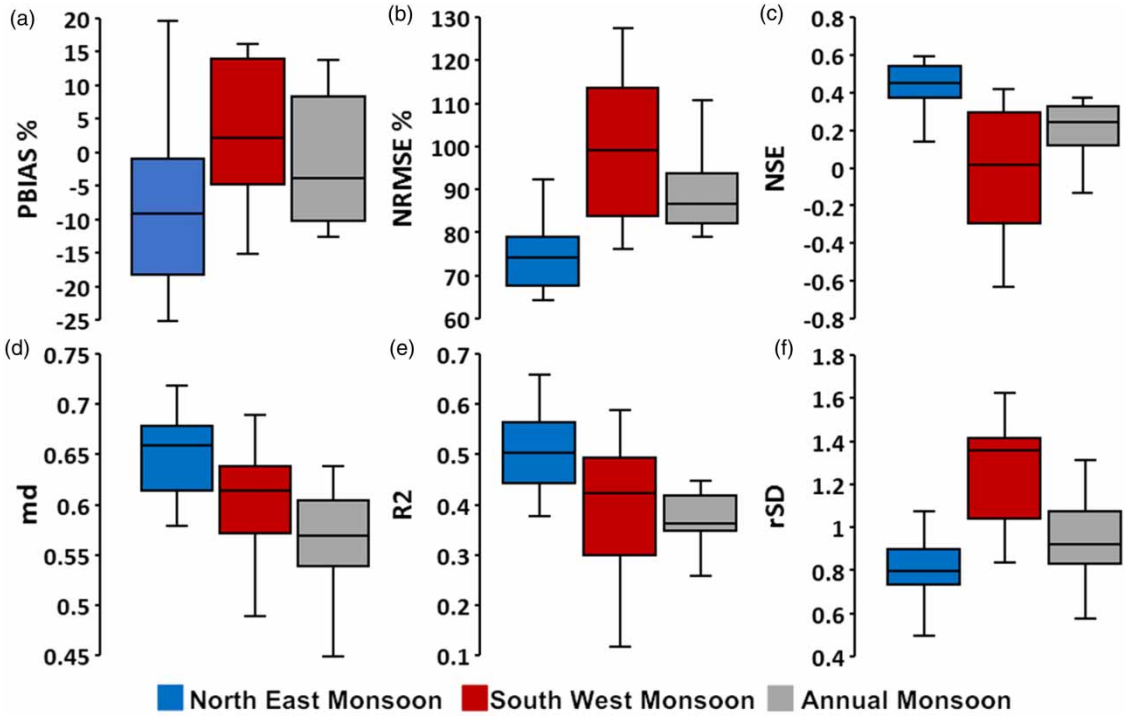

Figure 5 | The statistical evaluation results of the 20 GCMs against the 20CR rainfall estimates of the NEM, SWM and annual rainfall.

for each GCM and are presented in Table 3. The following equation presents an example of the CP calculation for BCC-CSM1.1(m):

$$L_{cp} = |0.08 - 0.00| + |0.73 - 0.64| + |0.47 - 0.59| + |0.66 - 0.72| + |0.52 - 0.67| + |0.91 - 0.97| = 0.55 \quad (9)$$

The Lcps of the NEM time frame range between 0.27 and 1.41. The CNRM-CM5 had the lowest Lcp of 0.27, indicating it as the closest GCM to 20CR estimates of historical NEM rainfall. On the contrary, the CMCC-CMS had the highest Lcp of 1.41, indicating it as the worst GCM in terms of simulating NEM rainfall. Based on the Lcp values, the GCMs were ranked ascendingly as shown in Table 3.

The same procedure was carried out for ranking GCMs in simulating rainfall for the SWM and annual time frames. Table 4 shows the final rank of GCMs in simulating spatial variability of NEM, SWM and annual rainfall in Peninsular Malaysia. As shown in the table, CMCC-CMS was ranked last for NEM, while it achieved the first position in simulating both SWM and annual rainfalls. This means, that the CMCC-CMS was able to simulate the annual and SWM rainfall spatial pattern very well, but completely failed in simulating NEM rainfall. Therefore, following the rule of thumb suggested by Ahmed *et al.* (2020), CMCC-CMS was discarded. A similar procedure was followed for all the GCMs and only the GCMs that achieved a rank between 1 and 10 for the three time frames were selected for the ensemble. This means that the final subset of GCMs should be able to simulate the annual and both monsoon rainfalls adequately. As shown in Table 4, two GCMs – BCC-CSM1-1 and HadGEM2-ES – showed acceptable performance for all the three time frames and were selected in the final subset of GCMs, although their individual ranks were not the highest. Therefore, those two GCMs were selected for future projection of rainfall in Peninsular Malaysia.

Bias correction of the selected GCMs

The selected GCMs, BCC-CSM1-1 and HadGEM2-ES, were bias-corrected using linear scaling method for the study area. Figure 6 shows scatter plots of the monthly raw and bias-corrected rainfall (presented by cross and circle

Table 3 | Results obtained using statistical metrics for assessment of the performance of GCMs in simulating NEM rainfall and the ranking of GCMs using compromised programming

Model	PBIAS	NRMSE	NSE	md	R^2	rSD	Lcp	Rank
BCC-CSM1.1(m)	0.08	0.73	0.47	0.66	0.52	0.91	0.55	8
BCC-CSM1 – 1	0.20	0.77	0.40	0.66	0.51	0.91	0.80	9
CanESM2	– 0.15	0.68	0.54	0.68	0.61	0.83	0.48	6
CCSM4	– 0.09	0.65	0.57	0.70	0.61	0.88	0.29	2
CMCC-CM	0.18	0.84	0.30	0.64	0.45	0.97	0.97	13
CMCC-CMS	0.17	0.92	0.14	0.59	0.41	1.08	1.41	20
CNRM-CM5	– 0.05	0.68	0.54	0.72	0.63	1.07	0.27	1
CSIRO-Mk3.6.0	– 0.20	0.76	0.43	0.61	0.52	0.5	1.20	17
GFDL-CM3	– 0.06	0.70	0.51	0.67	0.54	0.85	0.50	7
GISS-E2-H	– 0.25	0.75	0.44	0.63	0.58	0.54	1.11	16
HadGEM2-AO	– 0.13	0.73	0.47	0.66	0.50	0.71	0.83	12
HadGEM2-ES	– 0.09	0.74	0.46	0.66	0.47	0.73	0.81	11
INMCM4.0	– 0.18	0.64	0.59	0.70	0.67	0.76	0.41	4
MIROC5	– 0.18	0.85	0.28	0.58	0.39	0.78	1.30	19
MIROC-ESM	– 0.25	0.82	0.32	0.59	0.5	0.74	1.23	18
MIROC-ESM-CHEM	– 0.20	0.78	0.39	0.61	0.5	0.74	1.05	15
MPI-ESM-LR	– 0.11	0.79	0.37	0.63	0.42	0.81	0.98	14
MPI-ESM-MR	– 0.07	0.77	0.40	0.64	0.45	0.84	0.82	11
NorESM1-M	0.00	0.66	0.56	0.68	0.56	0.79	0.38	3
NorESM1-ME	– 0.03	0.67	0.55	0.68	0.55	0.79	0.44	5
Ideal value	**0.00**	**0.64**	**0.59**	**0.72**	**0.67**	**0.97**	–	–

Table 4 | The final rank of CGMs in estimating the rainfall amount at the NEM, SWM and annual time frames in Peninsular Malaysia

Model	NEM	SWM	Annual	Model	NEM	SWM	Annual
BCC-CSM1.1(m)	8	11	20	HadGEM2-AO	12	3	9
BCC-CSM1 – 1	**9**	**6**	**8**	**HadGEM2-ES**	**10**	**5**	**6**
CanESM2	6	12	4	INMCM4.0	4	18	11
CCSM4	2	10	15	MIROC5	19	8	14
CMCC-CM	13	2	3	MIROC-ESM	18	20	19
CMCC-CMS	20	1	1	MIROC-ESM-CHEM	15	19	18
CNRM-CM5	1	15	2	MPI-ESM-LR	14	7	12
CSIRO-Mk3.6.0	17	9	16	MPI-ESM-MR	11	4	5
GFDL-CM3	7	13	13	NorESM1-M	3	14	10
GISS-E2-H	16	17	17	NorESM1-ME	5	16	7

symbols, respectively) of the two GCMs against APHRODITE rainfall for the period 1961–2005. The figure clearly shows that the bias-corrected estimates having solid simple linear regression lines of the two GCMs are more aligned with the 1:1 diagonal line indicating the capability of linear scaling to bias correct the GCM raw rainfall. However, the bias-corrected rainfall was found to underestimate the higher rainfall and overestimate the lower rainfall

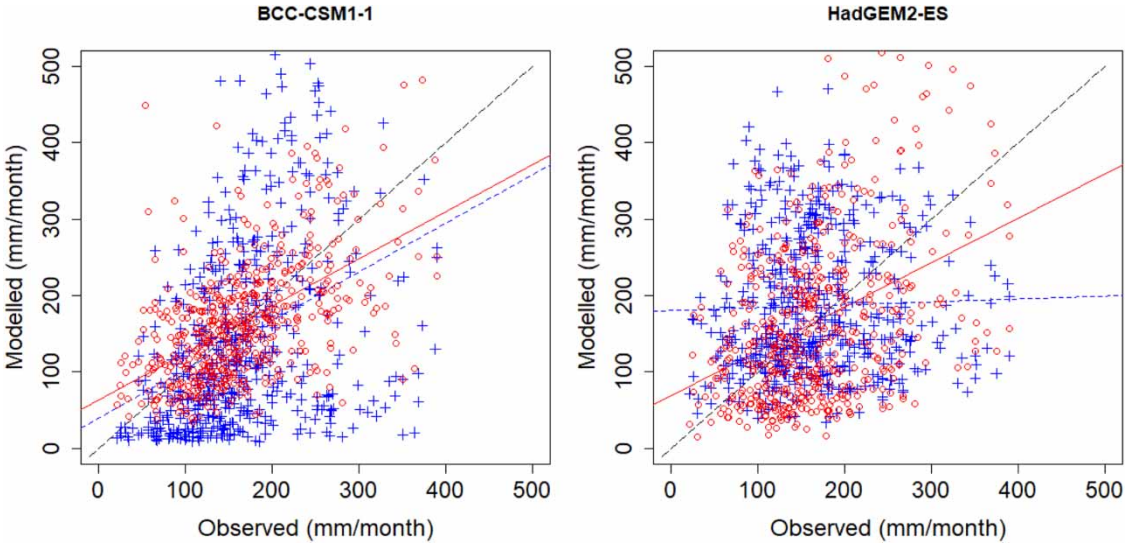

Figure 6 | Scatter plots of the monthly estimates of the raw (cross) and bias-corrected (circle) of the two selected GCMs, BCC-CSM1-1 (left panel) and HadGEM2-ES (right panel), against APHRODITE estimates for the historical period 1961–2005.

values. This is very common in bias correction of GCMs using any method (Ahmed *et al.* 2015). The bias correction factors obtained for the historical period (1961–2005) were used to correct the bias of the projected rainfall of the selected GCM for the period 2020–2099.

Spatial pattern of changes in the future rainfall in Peninsular Malaysia

The spatial distribution of the changes in daily rainfall can be helpful for better understanding of future rainfall variations in Peninsular Malaysia. Therefore, the changes in the mean, standard deviation and 95th percentile of daily rainfall for two future periods (near future: 2020–2059 and far future: 2060–2099) were calculated by comparing the future projections of the selected GCMs (i.e., BCC-CSM1-1 and HadGEM2-ES) for four RCPs with the historical simulation for the base period, 1971–2000. Then, maps were prepared to represent future changes in mean, variability and extreme rainfall.

Figure 7 presents the changes in the mean daily rainfall projected by the bias-corrected models, BCC-CSM1-1 and HadGEM2-ES, for the near and far futures under the four RCPs. The BCC-CSM1-1 projected an increase in the mean daily rainfall in the central region of the peninsular for the four RCPs during both future periods. This increase was as high as 10 mm in the central region during the far future for RCPs 2.6, 4.5 and 8.5. Furthermore, it projected a decrease in the mean daily rainfall in the far north and south of the peninsular during the two futures. The selected GCMs projected a decrease in rainfall by 10 mm in most of the peninsular for all the RCPs, with the highest decrease of −20 mm in the northwest for RCP 6.0.

The HadGEM2-ES model also projected an increase in the mean of the daily rainfall in the central regions under the four RCPs. However, HadGEM2-ES projected a decrease in the mean rainfall by 20 mm for the near and far futures in the south as well as the north of the peninsular. As shown in Figure 7, HadGEM2-ES showed contradictory projections of BCC-CSM1-1 in the north-west region as the former projected an increase in the mean rainfall by 20 mm.

Figure 8 shows the spatial variation of the standard deviation of annual rainfall projected by the bias-corrected GCMs, BCC-CSM1-1 and HadGEM2-ES, for the near and far future for the four RCPs. The BCC-CSM1-1 projected an increase in the rainfall standard deviation for entire Peninsular Malaysia under all RCPs. The highest increase was observed in the north of the peninsula at a rate of 40 mm during 2060–2099 for all the RCPs except RCP 6.0. On the other hand, the HadGEM2-ES estimated a decreasing pattern in the standard deviation of rainfall in the east of the peninsular. The maximum decrease was projected

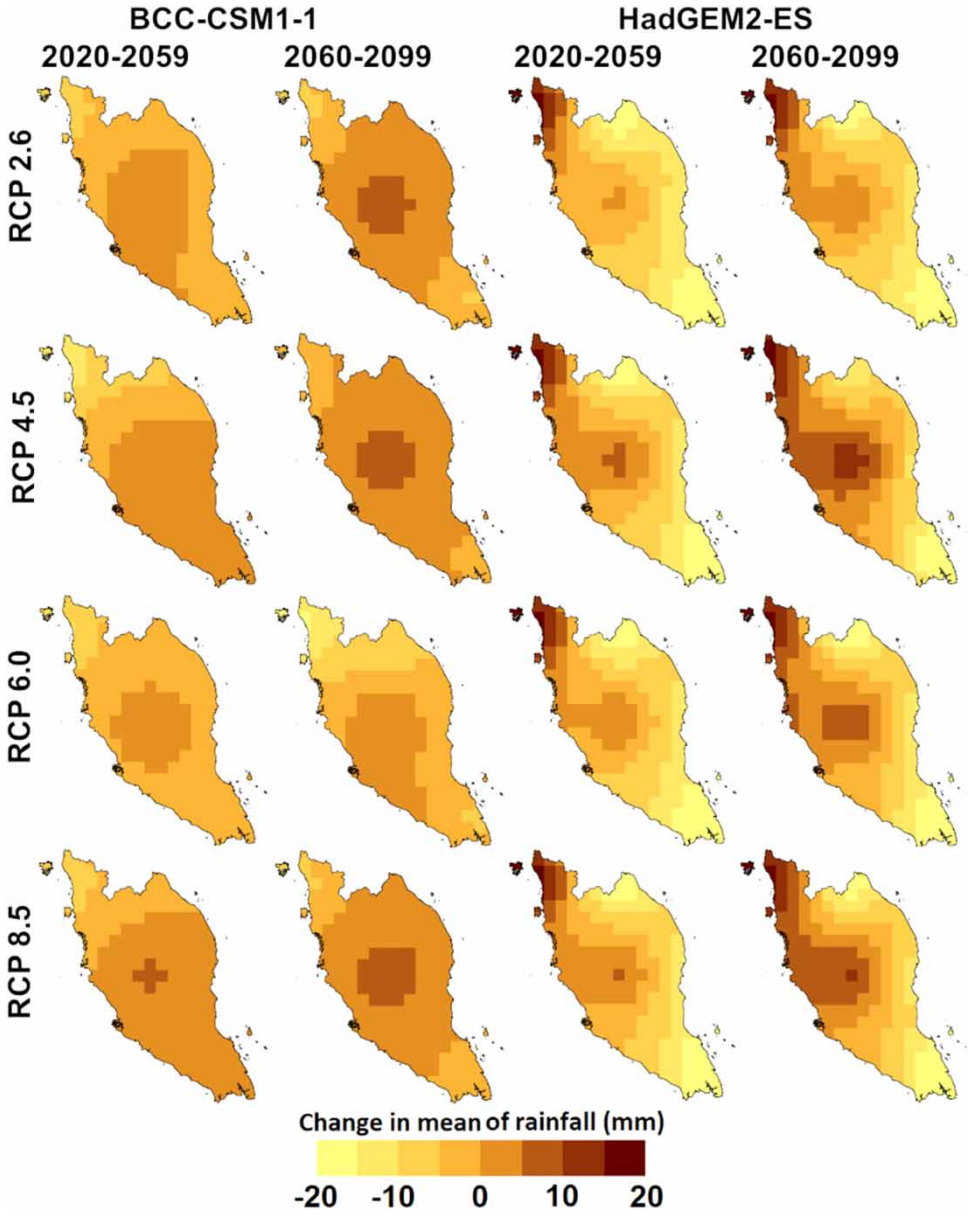

Figure 7 | Spatial distribution of the projected change in the annual mean rainfall in the near and far futures estimated by the bias-corrected GCMs, BCC-CSM1-1 and HadGEM2-ES, for different RCPs.

to reach up to −40 mm in the far south of the peninsular for all the four RCPs for both the near and the far futures. Furthermore, the HadGEM2-ES projected an increase in the standard deviation of the daily rainfall in the central and west regions which was also observed for BCC-CSM1-1 projections.

Figure 9 shows the spatial variation of changes in the 95th percentile rainfall amount projected by BCC-CSM1-1 and HadGEM2-ES for the near and far futures under different RCPs. The BCC-CSM1-1 projected an increase in the 95th percentile rainfall amount for the entire peninsular for all the RCPs. However, a slight decrease (−5 mm) in the far north-west and south-east was also projected. The highest projected increase in the 95th percentile rainfall amount was in the central region of the peninsular, by 25 mm during 2060–2099 for all RCPs. However, the HadGEM2-

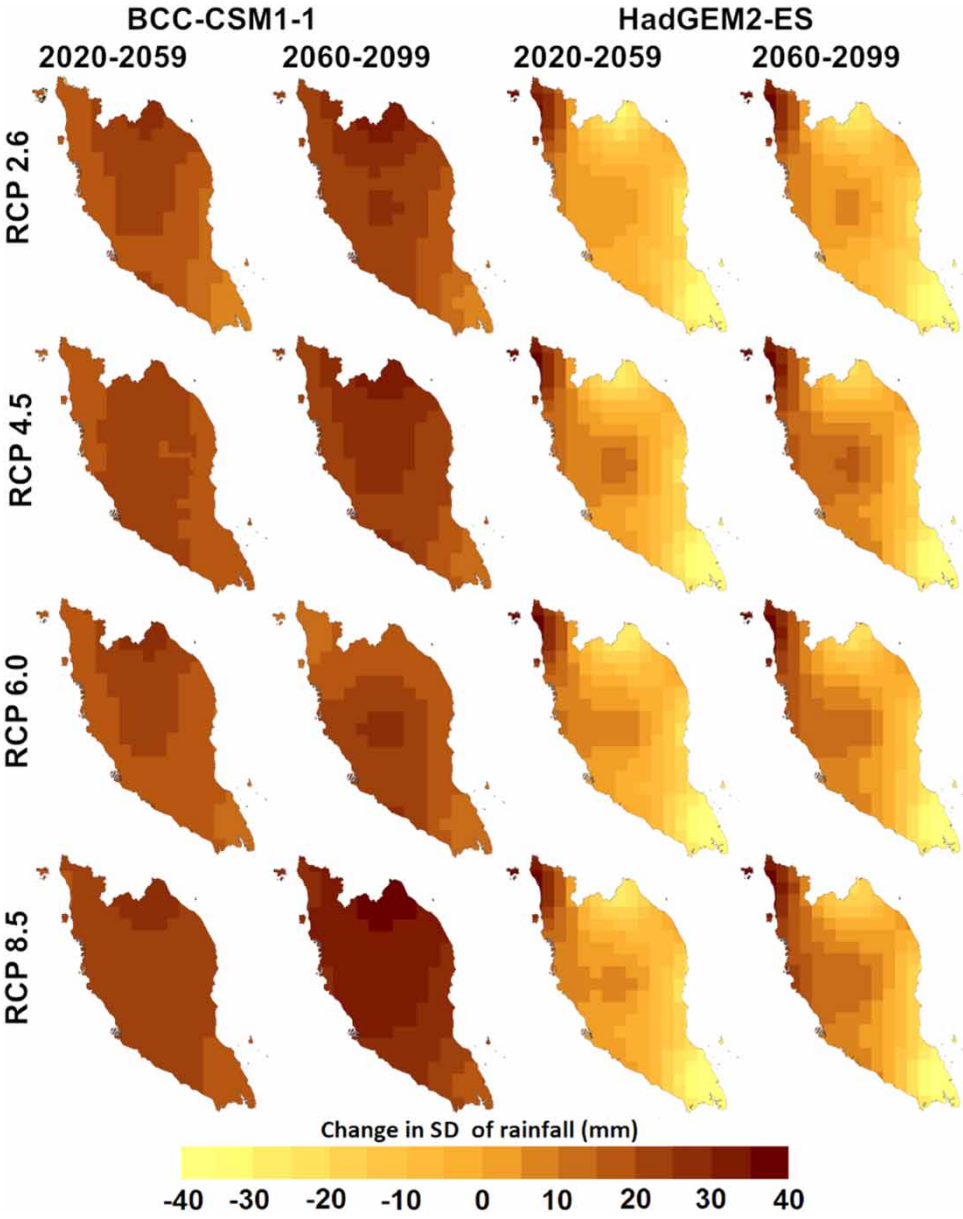

Figure 8 | Spatial distribution of the projected change in the standard deviation of annual rainfall in the near and far futures estimated by the bias-corrected GCMs, BCC-CSM1-1 and HadGEM2-ES, for different RCPs.

ES projected a decrease in the 95th percentile rainfall amount in the central and eastern regions of the Peninsular. The highest decrease was projected by −40 mm in the southwest tip. Furthermore, the HadGEM2-ES projected an increase in the north-west of the Peninsular by 25–35 mm. Overall, the extreme rainfall amount was found to change less in the south and north compared to central Peninsula Malaysia under BCC-CSM1-1, while there was an increase in the northwest and decrease in the central and east of Peninsular Malaysia for HadGEM2-ES.

CONCLUSION

An attempt has been made to reduce uncertainty in the projection of rainfall of Peninsular Malaysia through the

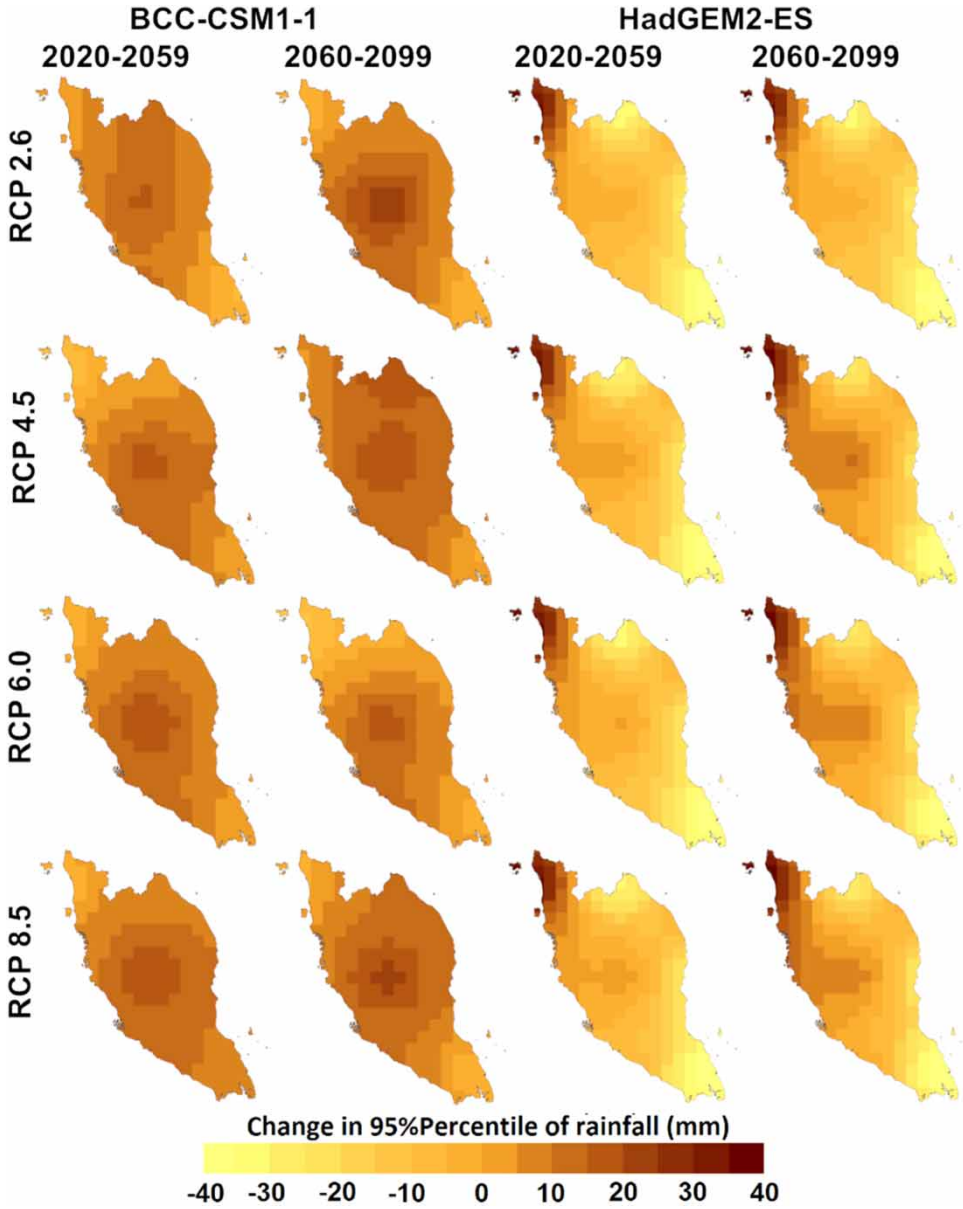

Figure 9 | Spatial distribution of the projected change in 95th percentile daily rainfall amount in the near and far futures estimated by the bias-corrected GCMs, BCC-CSM1-1 and HadGEM2-ES, for different RCPs.

selection of a credible subset of GCMs. The selection of GCMs was based on the hypothesis that the GCMs able to simulate the historical large-scale ocean-atmospheric phenomena responsible for climate variability of a region can be considered as more suitable for the projection of rainfall for the study area. Twenty GCMs' outputs of precipitation were evaluated using different statistical metrics and at three time frames during 1971–2005. Based on a compromise made among the evaluation metrics, this study found that two GCMs, namely, BCC-CSM1-1 and HadGEM2-ES, were the most credible for the projection of rainfall in Peninsular Malaysia. This finding agrees with the results of Noor *et al.* (2019b), where HadGEM2-ES was identified as one of the best four GCMs for the projection of daily rainfall in Peninsular Malaysia. The rainfall simulations of the two selected GCMs were then interpolated

to 0.25° × 0.25° and bias-corrected using APHRODITE as a reference dataset. Overall, the study revealed a projected increase in rainfall in the region where rainfall is usually less and a decrease in rainfall in the region where rainfall is usually high. This indicates more homogeneity in the spatial distribution of rainfall in the peninsula. BCC-CSM1-1 projected relatively less change in the south and north of the peninsular compared to the central region, while HadGEM2-ES projected an increase in rainfall in the northwest and a decrease in the central and eastern regions. The difference in projected rainfalls by the two GCMs indicates uncertainty in future rainfall. The uncertainty in projected rainfall was found higher in the region where annual rainfall is the highest (northern region) and lower where the annual rainfall is the lowest (central region). This is justifiable as higher uncertainty is usually associated with higher rainfall and vice versa. The study indicates that the selection of GCMs based on their consistency in simulating historical rainfall with observed rainfall does not guarantee their consistent future projections. This may be due to uncertainty in future climate in tropics under climate change scenarios. The large uncertainty in projections indicates more challenges in decision-making for adaptation to climate change in Peninsular Malaysia.

ACKNOWLEDGEMENT

The authors would like to acknowledge Universiti Teknologi Malaysia (UTM) for providing financial support for this research through RUG Grant Tier 2 Q.J130000.2622.14J27. S.S. and T.I. conceptualized the study, S.A.S., M.S.N. and S.S. performed the analysis; M.S.N. and S.S. wrote the original draft; M.S.N., S.S. and T.I. edited and revised the final draft. All authors have read and agreed to the published version of the manuscript.

REFERENCES

Ahmed, K., Shahid, S., Haroon, S. B. & Wang, X. J. 2015 Multilayer perceptron neural network for downscaling rainfall in arid region: a case study of Baluchistan, Pakistan. *Journal of Earth System Science* **124** (6), 1325–1341. doi:10.1007/s12040-015-0602-9.

Ahmed, K., Shahid, S., Nawaz, N. & Khan, N. 2019 Modeling climate change impacts on precipitation in arid regions of Pakistan: a non-local model output statistics downscaling approach. *Theoretical and Applied Climatology* **137** (1–2), 1347–1364. doi:10.1007/s00704-018-2672-5.

Ahmed, K., Sachindra, D. A., Shahid, S., Iqbal, Z., Nawaz, N. & Khan, N. 2020 Multi-model ensemble predictions of precipitation and temperature using machine learning algorithms. *Atmospheric Research* **236**, 104806. doi:10.1016/j.atmosres.2019.104806.

Aqilah Tukimat, N. N. 2018 Assessing the implementation of bias correction in the climate prediction. *IOP Conference Series: Materials Science and Engineering* **342**, 012004. doi:10.1088/1757-899x/342/1/012004.

Camici, S., Brocca, L., Melone, F. & Moramarco, T. 2014 Impact of climate change on flood frequency using different climate models and downscaling approaches. *Journal of Hydrologic Engineering* **19** (8), 04014002. doi:10.1061/(ASCE)HE.1943-5584.0000959.

Chen, W., Wiecek, M. M. & Zhang, J. 1999 Quality utility – a compromise programming approach to robust design. *Journal of Mechanical Design* **121** (2), 179–187. doi:10.1115/1.2829440.

Chen, T.-C., Tsay, J.-D., Yen, M.-C. & Matsumoto, J. 2013 The winter rainfall of Malaysia. *Journal of Climate* **26** (3), 936–958.

Deser, C., Phillips, A., Bourdette, V. & Teng, H. 2012 Uncertainty in climate change projections: the role of internal variability. *Climate Dynamics* **38** (3–4), 527–546.

Fang, G. H., Yang, J., Chen, Y. N. & Zammit, C. 2015 Comparing bias correction methods in downscaling meteorological variables for a hydrologic impact study in an arid area in China. *Hydrology and Earth System Sciences* **19** (6), 2547–2559. doi:10.5194/hess-19-2547-2015.

Gorantiwar, S. & Smout, I. K. 2010 Multicriteria decision making (compromise programming) for integrated water resources management in an irrigation scheme. In: *3rd International Perspective on Current & Future State of Water Resources & the Environment*. EWRI-ASCE, Chennai, India.

Harris, G. R., Sexton, D. M. H., Booth, B. B. B., Collins, M. & Murphy, J. M. 2013 Probabilistic projections of transient climate change. *Climate Dynamics* **40** (11), 2937–2972. doi:10.1007/s00382-012-1647-y.

Hewitt, J. E., Ellis, J. I. & Thrush, S. F. 2016 Multiple stressors, nonlinear effects and the implications of climate change impacts on marine coastal ecosystems. *Global Change Biology* **22** (8), 2665–2675. doi:10.1111/gcb.13176.

Hosseinzadehtalaei, P., Tabari, H. & Willems, P. 2017 Uncertainty assessment for climate change impact on intense precipitation: how many model runs do we need? *International Journal of Climatology* **37** (S1), 1105–1117. doi:10.1002/joc.5069.

Johnson, F. & Sharma, A. 2009 Measurement of GCM skill in predicting variables relevant for hydroclimatological

assessments. *Journal of Climate* **22** (16), 4373–4382. doi:10.1175/2009jcli2681.1.

Kaczmarska, J., Jewson, S. & Bellone, E. 2018 Quantifying the sources of simulation uncertainty in natural catastrophe models. *Stochastic Environmental Research and Risk Assessment* **32** (3), 591–605. doi:10.1007/s00477-017-1393-0.

Khan, N., Shahid, S., Ahmed, K., Ismail, T., Nawaz, N. & Son, M. 2018 Performance assessment of general circulation model in simulating daily precipitation and temperature using multiple gridded datasets. *Water* **10** (12), 1793. doi:10.3390/w10121793.

Lehner, F., Wood, A. W., Vano, J. A., Lawrence, D. M., Clark, M. P. & Mankin, J. S. 2019 The potential to reduce uncertainty in regional runoff projections from climate models. *Nature Climate Change* **9** (12), 926–933. doi:10.1038/s41558-019-0639-x.

Le Loh, J., Tangang, F., Juneng, L., Hein, D. & Lee, D.-I. 2016 Projected rainfall and temperature changes over Malaysia at the end of the 21st century based on PRECIS modelling system. *Asia-Pacific Journal of Atmospheric Sciences* **52** (2), 191–208.

Lenderink, G., van Ulden, A., van den Hurk, B. & Keller, F. 2007 A study on combining global and regional climate model results for generating climate scenarios of temperature and precipitation for the Netherlands. *Climate Dynamics* **29** (2), 157–176. doi:10.1007/s00382-007-0227-z.

Lutz, A. F., ter Maat, H. W., Biemans, H., Shrestha, A. B., Wester, P. & Immerzeel, W. W. 2016 Selecting representative climate models for climate change impact studies: an advanced envelope-based selection approach. *International Journal of Climatology* **36** (12), 3988–4005. doi:10.1002/joc.4608.

Mateus, C. & Tullos, D. 2017 Reliability, sensitivity, and uncertainty of reservoir performance under climate variability in basins with different hydrogeologic settings in Northwestern United States. *International Journal of River Basin Management* **15** (1), 21–37. doi:10.1080/15715124.2016.1247361.

Mayowa, O. O., Pour, S. H., Shahid, S., Mohsenipour, M., Harun, S. B., Heryansyah, A. & Ismail, T. 2015 Trends in rainfall and rainfall-related extremes in the east coast of peninsular Malaysia. *Journal of Earth System Science* **124** (8), 1609–1622.

McSweeney, C. F., Jones, R. G., Lee, R. W. & Rowell, D. P. 2015 Selecting CMIP5 GCMs for downscaling over multiple regions. *Climate Dynamics* **44** (11–12), 3237–3260. doi:10.1007/s00382-014-2418-8.

Muhammad, M. K. I., Nashwan, M. S., Shahid, S., Ismail, T., Song, Y. H. & Chung, E. S. 2019 Evaluation of empirical reference evapotranspiration models using compromise programming: a case study of Peninsular Malaysia. *Sustainability* **11** (16), 4267. doi:10.3390/su11164267.

Nash, J. E. & Sutcliffe, J. V. 1970 River flow forecasting through conceptual models part I – a discussion of principles. *Journal of Hydrology* **10** (3), 282–290. doi:10.1016/0022-1694(70)90255-6.

Nashwan, M. S. & Shahid, S. 2019 Symmetrical uncertainty and random forest for the evaluation of gridded precipitation and temperature data. *Atmospheric Research* **230**, 104632. doi:10.1016/j.atmosres.2019.104632.

Nashwan, M. S. & Shahid, S. 2020 A novel framework for selecting general circulation models based on the spatial patterns of climate. *International Journal of Climatology*. doi:10.1002/joc.6465.

Nashwan, M. S., Ismail, T. & Ahmed, K. 2018a Flood susceptibility assessment in Kelantan river basin using copula. *International Journal of Engineering and Technology* **7** (2), 584–590. doi:10.14419/ijet.v7i2.10447.

Nashwan, M. S., Shahid, S., Chung, E. S., Ahmed, K. & Song, Y. H. 2018b Development of climate-based index for hydrologic hazard susceptibility. *Sustainability* **10** (7), 2182. doi:10.3390/su10072182.

Nashwan, M. S., Ismail, T. & Ahmed, K. 2019a Non-stationary analysis of extreme rainfall in Peninsular Malaysia. *Journal of Sustainability Science and Management* **14** (3), 17–34.

Nashwan, M. S., Shahid, S. & Wang, X. J. 2019b Uncertainty in estimated trends using gridded rainfall data: a case study of Bangladesh. *Water* **11** (2), 349. doi:10.3390/w11020349.

Noor, M., Ismail, T., Chung, E.-S., Shahid, S. & Sung, J. 2018 Uncertainty in rainfall intensity duration frequency curves of Peninsular Malaysia under changing climate scenarios. *Water* **10** (12), 1750.

Noor, M., Ismail, T., Shahid, S., Nashwan, M. S. & Ullah, S. 2019a Development of multi-model ensemble for projection of extreme rainfall events in Peninsular Malaysia. *Hydrology Research* **50** (6), 1772–1788. doi:10.2166/nh.2019.097.

Noor, M., Ismail, T., Shahid, S., Ahmed, K., Chung, E.-S. & Nawaz, N. 2019b Selection of CMIP5 multi-model ensemble for the projection of spatial and temporal variability of rainfall in peninsular Malaysia. *Theoretical and Applied Climatology* **138**, 999–1012. doi:10.1007/s00704-019-02874-0.

Pour, S. H., Bin Harun, S. & Shahid, S. 2014 Genetic programming for the downscaling of extreme rainfall events on the east coast of Peninsular Malaysia. *Atmosphere* **5** (4), 914–936. doi:10.3390/atmos5040914.

Pour, S. H., Shahid, S., Chung, E. S. & Wang, X. J. 2018 Model output statistics downscaling using support vector machine for the projection of spatial and temporal changes in rainfall of Bangladesh. *Atmospheric Research* **213**, 149–162. doi:10.1016/j.atmosres.2018.06.006.

Pour, S. H., Wahab, A. K. A. & Shahid, S. 2020 Physical-empirical models for prediction of seasonal rainfall extremes of Peninsular Malaysia. *Atmospheric Research* **233**, 104720.

Qin, X. S. & Lu, Y. 2014 Study of climate change impact on flood frequencies: a combined weather generator and hydrological modeling approach. *Journal of Hydrometeorology* **15** (3), 1205–1219. doi:10.1175/jhm-d-13-0126.1.

Raju, K. S., Sonali, P. & Kumar, D. N. 2017 Ranking of CMIP5-based global climate models for India using compromise programming. *Theoretical and Applied Climatology* **128** (3–4), 563–574. doi:10.1007/s00704-015-1721-6.

Rezaei, F., Ahmadzadeh, M. R. & Safavi, H. R. 2017 SOM-DRASTIC: using self-organizing map for evaluating groundwater potential to pollution. *Stochastic Environmental Research and Risk Assessment* **31** (8), 1941–1956. doi:10.1007/s00477-016-1334-3.

Sa'adi, Z., Shahid, S., Ismail, T., Chung, E.-S. & Wang, X.-J. 2017 Trends analysis of rainfall and rainfall extremes in Sarawak, Malaysia using modified Mann–Kendall test. *Meteorology and Atmospheric Physics* 1–15. doi:10.1007/s00703-017-0564-3.

Sa'adi, Z., Shiru, M. S., Shahid, S. & Ismail, T. 2019 Selection of general circulation models for the projections of spatio-temporal changes in temperature of Borneo Island based on CMIP5. *Theoretical and Applied Climatology*. doi:10.1007/s00704-019-02948-z.

Sachindra, D. A., Ahmed, K., Rashid, M. M., Shahid, S. & Perera, B. J. C. 2018 Statistical downscaling of precipitation using machine learning techniques. *Atmospheric Research* **212**, 240–258. doi:10.1016/j.atmosres.2018.05.022.

Sachindra, D. A., Ahmed, K., Rashid, M. M., Sehgal, V., Shahid, S. & Perera, B. J. C. 2019 Pros and cons of using wavelets in conjunction with genetic programming and generalised linear models in statistical downscaling of precipitation. *Theoretical and Applied Climatology*. doi:10.1007/s00704-019-02848-2.

Salman, S. A., Shahid, S., Ismail, T., Ahmed, K. & Wang, X. J. 2018 Selection of climate models for projection of spatiotemporal changes in temperature of Iraq with uncertainties. *Atmospheric Research* **213**, 509–522. doi:10.1016/j.atmosres.2018.07.008.

Salman, S. A., Shahid, S., Ismail, T., Al-Abadi, A. M., Wang, X. J. & Chung, E. S. 2019 Selection of gridded precipitation data for Iraq using compromise programming. *Measurement* **132**, 87–98. doi:10.1016/j.measurement.2018.09.047.

Satoh, M., Noda, A. T., Seiki, T., Chen, Y.-W., Kodama, C., Yamada, Y., Kuba, N. & Sato, Y. 2018 Toward reduction of the uncertainties in climate sensitivity due to cloud processes using a global non-hydrostatic atmospheric model. *Progress in Earth and Planetary Science* **5** (1), 67. doi:10.1186/s40645-018-0226-1.

Shahid, S., Pour, S. H., Wang, X. J., Shourav, S. A., Minhans, A. & Ismail, T. 2017 Impacts and adaptation to climate change in Malaysian real estate. *International Journal of Climate Change Strategies and Management* **9** (1), 87–103. doi:10.1108/Ijccsm-01-2016-0001.

Shiogama, H., Stone, D., Emori, S., Takahashi, K., Mori, S., Maeda, A., Ishizaki, Y. & Allen, M. R. 2016 Predicting future uncertainty constraints on global warming projections. *Scientific Reports* **6** (1), 18903. doi:10.1038/srep18903.

Shiru, M. S., Shahid, S., Chung, E. S., Alias, N. & Scherer, L. 2019 A MCDM-based framework for selection of general circulation models and projection of spatio-temporal rainfall changes: a case study of Nigeria. *Atmospheric Research* **225**, 1–16. doi:10.1016/j.atmosres.2019.03.033.

Tan, M. L., Ibrahim, A. L., Duan, Z. P., Cracknell, A. & Chaplot, V. 2015 Evaluation of six high-resolution satellite and ground-based precipitation products over Malaysia. *Remote Sensing* **7**, 1504–1528. doi:10.3390/rs70201504.

Tan, M. L., Gassman, P. W. & Cracknell, A. P. 2017 Assessment of three long-term gridded climate products for hydro-climatic simulations in tropical river basins. *Water* **9** (3), 229.

Weigel, A. P., Knutti, R., Liniger, M. A. & Appenzeller, C. 2010 Risks of model weighting in multimodel climate projections. *Journal of Climate* **23** (15), 4175–4191. doi:10.1175/2010jcli3594.1.

Willmott, C. J. 2013 On the validation of models. *Physical Geography* **2** (2), 184–194. doi:10.1080/02723646.1981.10642213.

Yatagai, A., Kamiguchi, K., Arakawa, O., Hamada, A., Yasutomi, N. & Kitoh, A. 2012 APHRODITE constructing a long-term daily gridded precipitation dataset for Asia based on a dense network of rain gauges. *Bulletin of the American Meteorological Society* **93** (9), 1401–1415. doi:10.1175/Bams-D-11-00122.1.

Yen, M.-C., Chen, T.-C., Hu, H.-L., Tzeng, R.-Y., Dinh, D. T., Nguyen, T. T. T. & Wong, C. J. 2011 Interannual variation of the fall rainfall in Central Vietnam. *Journal of the Meteorological Society of Japan. Series II* **89**, 259–270.

Zeleny, M. 1973 Compromise programming, multiple criteria decision-making. In: *Multiple Criteria Decision Making* (M. Zeleny & J. L. Cochrane, eds). University of South Carolina Press, Columbia, SC, USA, pp. 263–301.

First received 20 September 2019; accepted in revised form 17 April 2020. Available online 19 June 2020